Observation of Ballooning Instabilities with Medium Toroidal Mode Number in High Temperature Tokamak Plasmas

PPPL--2850

DE92 018962

Y. Nagayama[a)], S. A. Sabbagh[b,c)], J. Manickam, E. D. Fredrickson, M. Bell, R.V. Budny, A. Cavallo[d)], A. C. Janos, M. E. Mauel[b)], K. M. McGuire, G. A. Navratil[b)], G. Taylor, and M. Yamada

Princeton Plasma Physics Laboratory, Princeton University
Princeton, New Jersey 08543

Abstract

A beta degradation event in a high β_p, TFTR tokamak plasma is analyzed with X-ray and electron cyclotron emission (ECE) imaging techniques. Medium-n (toroidal mode number) instabilities with ballooning characteristics are observed near and within the q =1.5 surface during a slow degradation in the plasma β and precede a sudden partial collapse in the central plasma pressure. This is the first reported observation of a ballooning instability in the interior of a large, collisionless tokamak plasma.

[a)]Present address: University of Tsukuba, Ibaraki 305, Japan

[b)]Columbia University, New York, N.Y. 10027

[c)]Present address: Plasma Physics Laboratory, Princeton University

[d)]Present address: Center for Energy and Environment Studies, Princeton University

The economic feasibility of tokamaks as fusion reactors is strongly dependent on the maximum value of β (the ratio of plasma to magnetic field pressure) that can be achieved in these devices. The β in present tokamak experiments is limited by fast disruptions that terminate the discharge, or by instabilities that either suddenly or gradually degrade the plasma confinement. Empirically, it has been found that the maximum β obtained in tokamaks is consistent with the Troyon limit [1], $\beta_{max} = 3 \times 10^{-8}\, I(\mathrm{A})/a(\mathrm{m})B(\mathrm{T})$, which is derived from a combination of experimental data and theoretically predicted instability thresholds for ideal magnetohydrodynamic (MHD) kink and ballooning modes. However, ballooning instabilities, which theoretically have fast growth times ($\sim 10\ \mu$s) and short wavelengths perpendicular to the magnetic field, have not yet been observed and identified in large tokamak experiments.

A significant result of the present work is the observation of medium-n, ($4 \leq n \leq 10$) ballooning modes that appear in a series of discharges in TFTR designed to achieve high β_p ($\beta_p \geq 2$) operation [2]. The modes occur during a slow degradation in the plasma β and precede a sudden partial collapse in the central plasma pressure. The amplitude of the mode is larger on the outboard (low-field) side of the torus and has a fast growth rate, characteristic of an ideal MHD ballooning instability. While high-n ballooning modes were observed in a small, short pulse-length resistive plasma in TORUS II [3], this is the first reported observation of a ballooning mode in the interior of a large, collisionless tokamak plasma.

Figure 1 shows the time evolution of plasma parameters for two high β_p plasmas, one with, and one without a degradation in poloidal beta. The plasmas were created by rapidly decreasing the plasma current prior to neutral beam injection. The discharge heated with 18 MW of power (shot 54018) experiences a gradual degradation in β_p beginning at $t = 3.77$ s, and a sudden collapse in the central density at $t = 3.78$ s. MHD oscillations are also greatly enhanced at this time, leading to a reduction in plasma confinement. The other discharge shown does not suffer a similar reduction in plasma parameters. This plasma has the same evolution of total current, but is heated with only 15 MW of neutral beam power.

The time evolution of the electron temperature profile and the soft X-ray emission profile at the moment of the β collapse is shown in Fig. 2. The electron cyclotron emission (ECE) is measured with a 20 channel grating polychromator which is cross-calibrated to a Michelson interferometer [4]. The data is collected with a 2 μs time resolution covering the major radius from $R = 2.3$ - 3.3 m. The channel separation is 6cm with a radial resolution of 3 cm. The soft X-rays are detected with a vertical camera (20 detectors) and a horizontal camera (60 detectors) [5]. It is useful to subtract the time averaged part from the total ECE signal and view the perturbation profile, Fig. 2(b). The contour plot of the perturbation amplitude provides a visual representation of the instabilities and facilitates identification of the location and relative spatial intensity of the oscillations [6].

The slow degradation in β_p begins at 3.7 s with the growth of an $(m, n) = (3, 2)$ mode. The (3, 2) mode has only a weak effect on confinement. About 80 ms later, (at $t = 3.7799$ s) a fast drop in the central electron temperature occurs. Hereafter, we will reference times from $t = 3.7795$ s, defining $\Delta t = t - 3.7795$ s. A second, higher frequency mode starts to grow at $\Delta t = 0.14$ ms. These modes are located near the radius of the (3, 2) mode. After the onset of the higher frequency mode, the MHD activity expands inward. At $\Delta t = 0.3$ ms, a strong $n = 6$ mode appears and the flattening of the temperature profile near the $q = 1.5$ surface is completed. During the crash ($\Delta t = 0.35$ - 0.43 ms), a (1, 1) mode appears and the central electron temperature decreases. Following the crash, the (3, 2) mode appears along with the (1, 1) mode. The medium-n mode has a growth time of less than 20 μs. This last mode shows a strong inside/outside asymmetry with a larger amplitude on the weak field side as might be expected for a ballooning mode [see Figs. 2 and 3(e)]. A similar instability has been observed in other TFTR discharges (about 20) for which the fast time resolution ECE data has been analyzed. A summary of a few of these shots is given in Table 1.

The ballooning mode is not detectable on the Mirnov coil system, thus the usual method of identifying mode numbers cannot be used. Identification of the toroidal mode number is made by taking advantage of the 18° separation of the horizontal X-ray camera and the grating polychromator. Comparison of the ECE profile and the horizontal X-ray profile gives $n = 6 \pm 1$.

The poloidal mode number of a helical instability in a tokamak plasma can be estimated by simulating the X-ray emission of a perturbed model source function [7]. By rotating the model X-ray source function toroidally at the proper frequency, the simulated signals can be compared with the actual signals to obtain the m number for the observed $n = 6$ instability (Fig. 3). The experimental data describing the initial growth of the mode is well modelled by invoking a helical "wave packet" perturbation that is localized in the poloidal and toroidal directions. The best agreement is obtained between the simulation and experiment when a perturbation with $m = 7 \pm 2$ is used [see Fig. 3(b, d)], but whose amplitude is significant over approximately 3/7 of the poloidal cross section. The terminology "(m, n)=(7, 6) wave packet" means that the instability has a (7, 6) helical structure. This source function model is shown in various phases in Fig. 3(f, g) corresponding to the times shown in Fig. 3(b, d). Obtaining agreement with the measured signals also requires that the Shafranov shift of the magnetic axis is included and that the localized perturbation amplitude of the mode increases when it resides on the weak field side of the torus [shown in Fig. 3(g)], characteristic of a ballooning instability. The maximum peak-to-peak amplitude of the experimentally measured soft X-ray fluctuation level [Fig. 3(e)] exhibits a similar ballooning feature.

These discharges have been modelled using the TRANSP code [8]. The equilibrium representing the plasma prior to the degradation in β_p was computed by a two-dimensional flux-coordinate equilibrium solver using the radial pressure, q profiles and outer boundary information taken from the TRANSP simulation. At t = 3.75 s, the central q value was 1.28, the edge q was 14.7, and a region of low shear was present near q = 1.5. The pressure profile was peaked, with the ratio of central to volume averaged pressure being 5.5. Although the simulated profiles near the magnetic axis are uncertain, the absence of sawtooth activity gives credence to modelling $q_0 > 1$.

The stability to both kink and ballooning modes was computed for these equilibria. It is found that prior to the sharp drop in the central pressure, the plasma is close to the threshold for instability to high-n ballooning modes. The computed equilibrium remains stable (near marginal stability) when q_0 is reduced from 1.28 to 1 [Fig. 4(a)]. Stability to low-n ideal MHD modes was determined using the PEST code [9]. The plasma was computed to be stable to the $n = 1$ external kink mode and unstable to an $n = 6$ internal ballooning mode. The peaked pressure and low shear near the magnetic axis suggest that the instability is of the infernal type [10]. This was verified by examining the stability while varying the toroidal mode number. The dependence of the growth rate on n has the oscillatory behavior typical of infernal modes. A similar resonant behavior is expected if q_0 is varied, with different m/n numbers being unstable [Fig. 4(b)]. The instabilities have predicted growth-times in the range of $10 \rightarrow 50\ \mu s$, which compare quite well to the observed values.

A major difficulty in equilibrium and stability analysis of this type is the experimental uncertainty in the plasma pressure profile (especially the nonthermal component) and the q profile. Efforts to obtain detailed measurements of the equilibrium q profiles will be carried out in the future to improve the comparison between theory and experiment.

In summary, ballooning modes of medium-n value have been observed in high β_p plasmas with pressure gradients calculated to be near the first stability boundary. The following observations support the identification of these modes as ballooning modes: (1) the identified toroidal mode numbers ($4 \leq n \leq 10$) are much higher than the usual kink or tearing mode, (2) the modes are stronger on the weak field side of the torus (i.e., they exhibit a strong ballooning characteristic), (3) the growth rate of the modes is consistent with the calculated ballooning mode growth rate using linear ideal MHD stability theory, and (4) reconstruction of the plasma equilibrium shows the pressure gradient to be near the first stability boundary and unstable to infernal-type ballooning modes.

Acknowledgements

The authors would like to thank Dr. M. Phillips of the Grumman Corporation for the use of equilibrium and stability codes. Dr. H. Park for the electron density measurement, and Drs. M. Chance, M. Okabayashi and W. Park for useful discussions. This work was supported by the U.S. Department of Energy under contract No. DE-AC02-76-CHO-3073 and DE-FG02-89ER53297.

References

[1] F. Troyon et al., Plasma Physics and Controlled Fusion **26**, 209 (1984).

[2] S. A. Sabbagh et al., Phys. Fluids B **3**, 2277 (1991).

[3] M. Machida and G.A. Navratil, Phys. Rev. Lett. **51**, 992 (1983).

[4] A. Cavallo et al., Rev. Sci. Instrum. **59**, 889 (1988). F. J. Stauffer et. al., *ibid.* **59**, 2139 (1988).

[5] K. W. Hill et al., Rev. Sci. Instrum. **56**, 830 (1985). L. C. Johnson et al., *ibid.* **57**, 2133 (1986).

[6] Y. Nagayama et al., Phys. Rev. Lett. **67**, 3527 (1991).

[7] S. Tsuji et al., Nucl. Fusion **25**, 305 (1985).

[8] R. J. Hawryluk, in Physics of Plasma Close to Thermonuclear Conditions, edited by B. Coppi et al., (Commission of the European Communities, Brussels, 1980), Vol.**1**, p.19.

[9] R. Grimm, R.L. Dewar and J. Manickam, J. Comput. Phys. **49**, 94 (1983).

[10] J. Manickam, N. Pomphrey and A. M. M. Todd, Nucl. Fusion **27**, 461 (1987).

Figure Captions

FIG. 1.
Summary of the time dependence of various plasma parameters for two high β_p discharges. The solid line indicates the beta degradation case (shot 54018) and the broken line indicates a case in which β_p saturates (shot 54013). The vertical arrow indicates the time at which the ballooning mode is observed.

FIG. 2.
Contour plots of the time evolution of the ECE profile in shot 54018: (a) electron temperature profile; the contour step size is 300 eV, (b) perturbation of ECE signal, (c) chord integrated soft X-ray emission profile (horizontal view).

FIG. 3.
Comparison of observed soft X-ray signals and the signals simulated by the model source function: (a) the observed soft X-ray signals from the horizontal camera, (b) the simulated waveforms from the horizontal camera by the (m, n)=(7, 6) model, (c) the observed soft X-ray signals from the vertical camera, (d) the simulated waveforms from the vertical camera by the (7, 6) model, (e) maximum peak-to-peak amplitude of the fluctuation between 3.77977s and 3.77984s, where the hatched area is the base fluctuation level which is sampled between 3.7794s and 3.7796s, (f) "wave packet" model source function at time "A", (g) "wave packet" model source function at time "B". The times "A" and "B" are shown in frames (b) and (d). Note that the amplitude of the perturbation has increased as it has moved to the weak field side of the torus.

FIG. 4.
(a) High-n ballooning stability for high-β_p discharge 54018. The solid line indicates the equilibrium pressure gradient at t = 3.75s. The enclosed

region is unstable to high-n ballooning modes. The pressure gradients are plotted vs. the square root of the normalized poloidal flux, which corresponds to the minor radius. (b) Growth rate of infernal modes with various toroidal mode numbers vs. q_0. The values are normalized to the poloidal Alfven frequency.

TFTR Shot No.	β_p	q_a	precursor (m, n)	Ballooning mode n	$\tau(\mu s)$
44677	1.3	5.9	not clear	4	50
53356	1.6	4.9	(3, 2)	6	80
54017	1.9	7.5	(4, 3)	3	20
54018	2.1	7.6	(3, 2)	6	30
54021	2.2	7.5	(3, 2)	6	20

TABLE I. Summary of discharges in which medium-n modes are observed. The toroidal mode number of the ballooning instability, the growth time and the precursor mode are given, along with the plasma edge safety factor and β_p. The mode growth time generally decreases as the β_p increases.

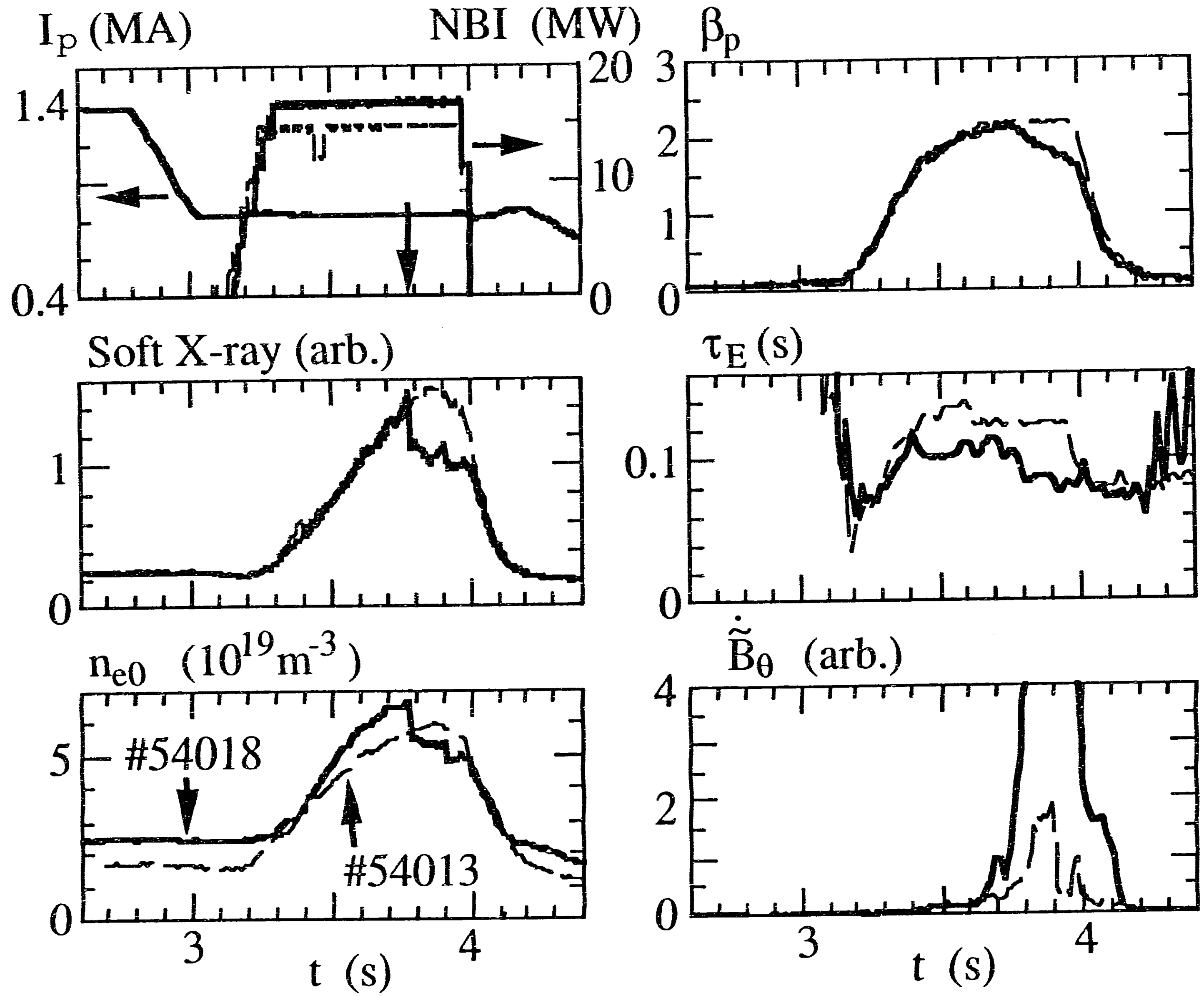
I_p (MA)
NBI (MW)
β_p
Soft X-ray (arb.)
τ_E (s)
n_{e0} ($10^{19}m^{-3}$)
#54018
#54013
$\dot{\tilde{B}}_\theta$ (arb.)
t (s)
t (s)

Fig. 1

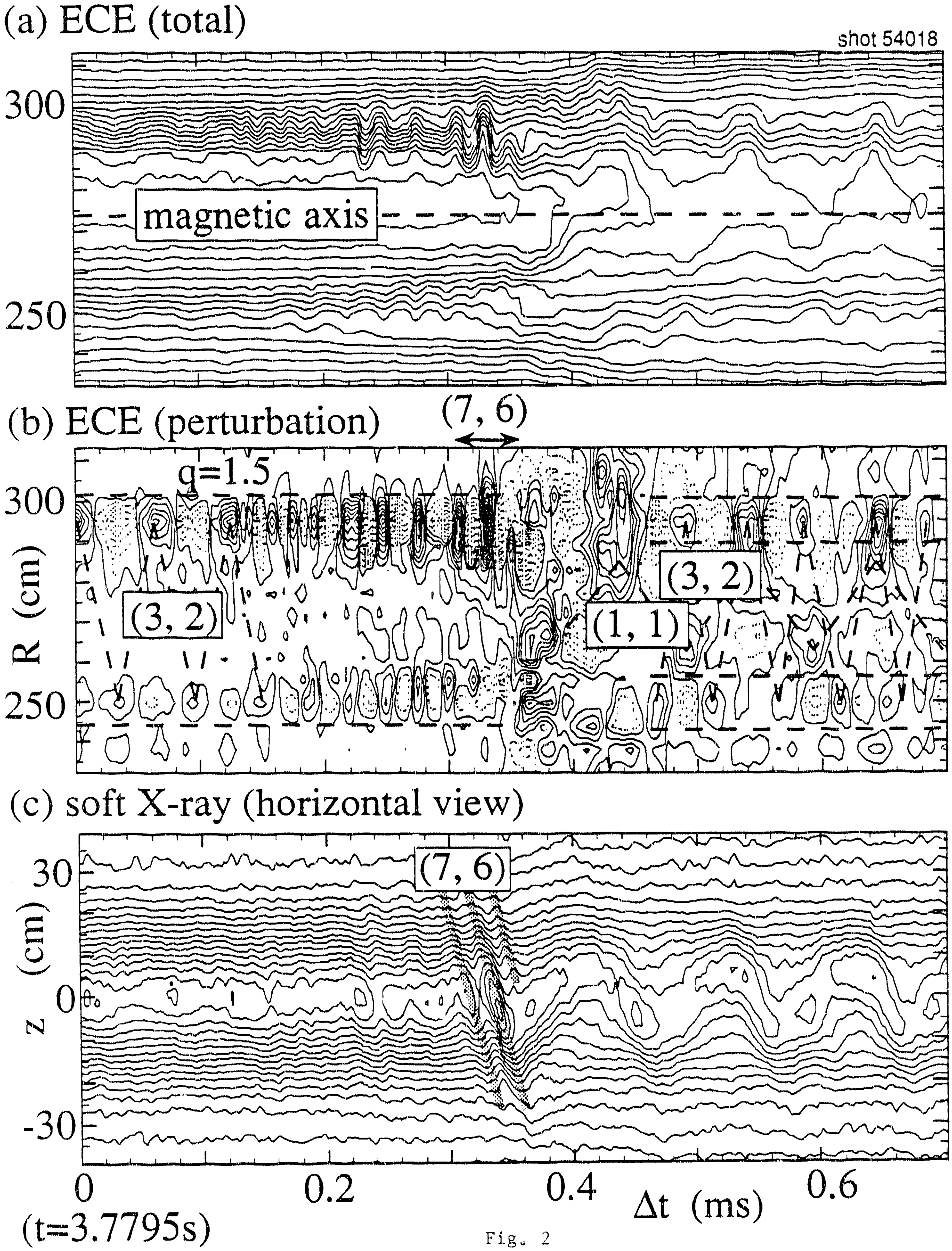
(a) ECE (total)
shot 54018
300
magnetic axis
250
(b) ECE (perturbation)
(7, 6)
q=1.5
300
R (cm)
(3, 2)
(3, 2)
(1, 1)
250
(c) soft X-ray (horizontal view)
(7, 6)
30
z (cm)
0
-30
0
0.2
0.4
Δt (ms)
0.6
(t=3.7795s)

Fig. 2

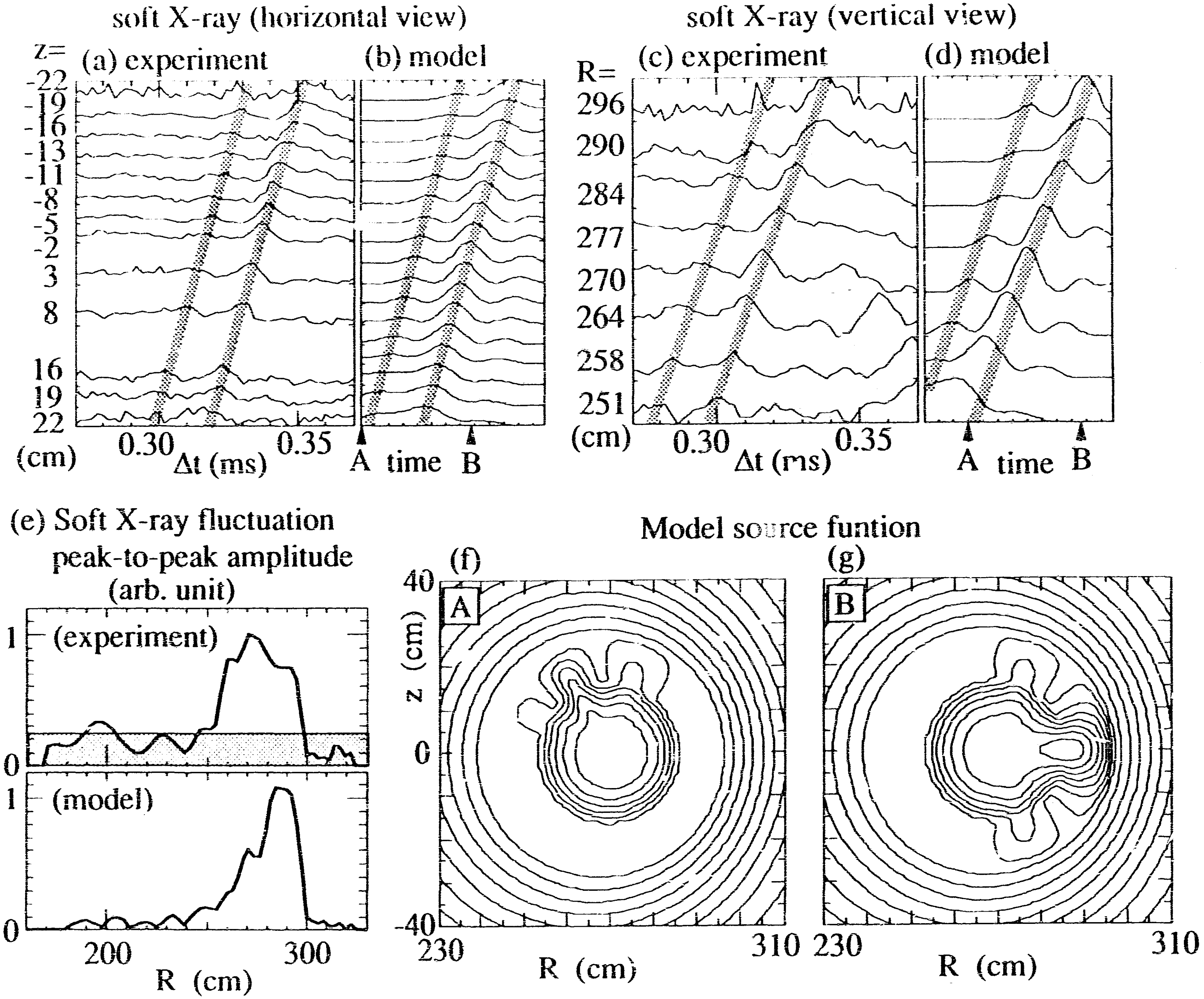

soft X-ray (horizontal view)
(a) experiment
(b) model
z=
-22
-19
-16
-13
-11
-8
-5
-2
3
8
16
19
22
(cm)
0.30
0.35
Δt (ms)
A time B
soft X-ray (vertical view)
(c) experiment
(d) model
R=
296
290
284
277
270
264
258
251
(cm)
0.30
0.35
Δt (ms)
A time B
(e) Soft X-ray fluctuation
peak-to-peak amplitude
(arb. unit)
(experiment)
(model)
1
0
200
300
R (cm)
Model source funtion
(f)
(g)
A
B
40
0
-40
z (cm)
230
310
R (cm)

Fig. 3

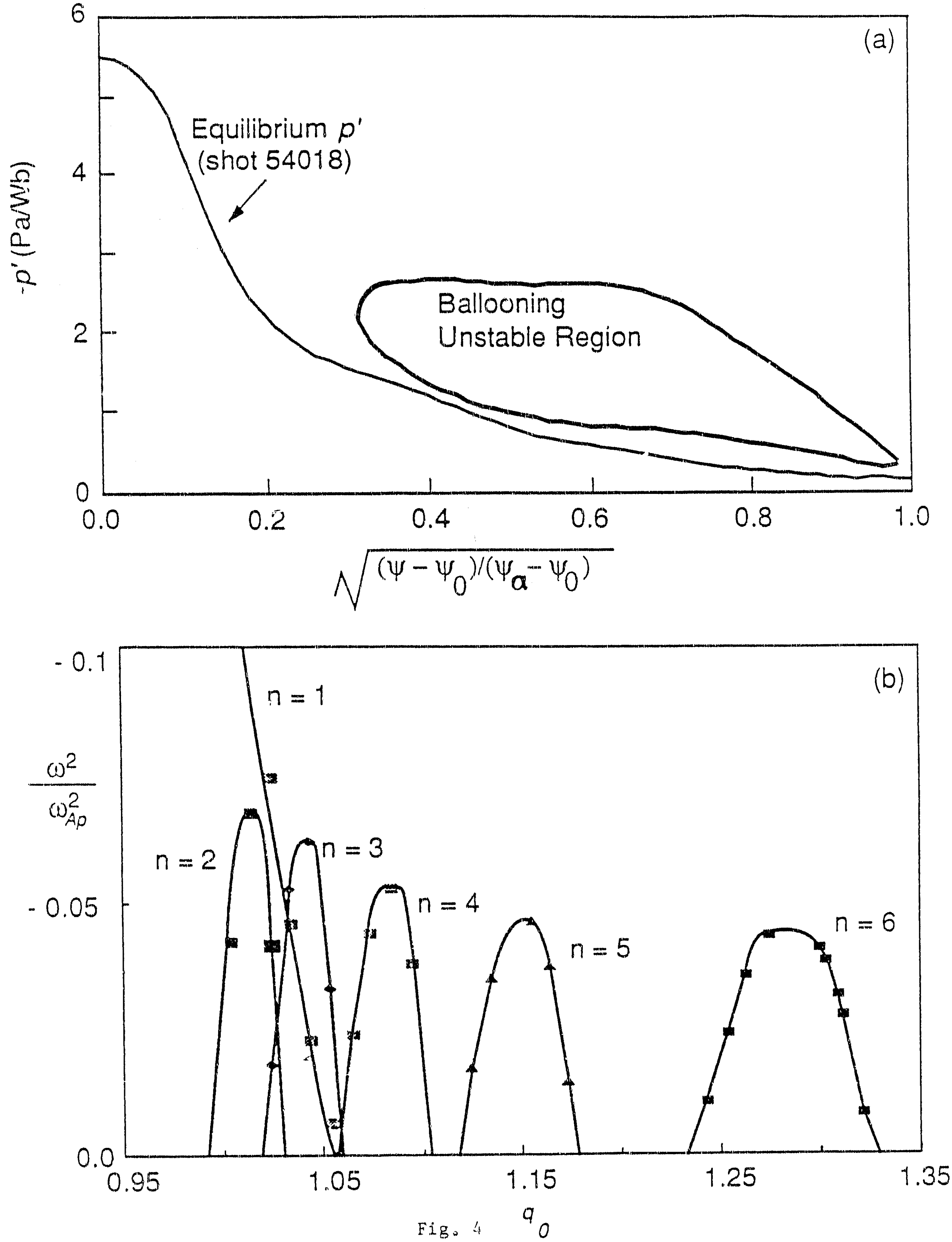
(a)
Equilibrium p'
(shot 54018)
Ballooning
Unstable Region
-p' (Pa/Wb)
0.0
0.2
0.4
0.6
0.8
1.0
(b)
n = 1
n = 2
n = 3
n = 4
n = 5
n = 6
- 0.1
- 0.05
0.0
0.95
1.05
1.15
1.25
1.35
q0

Fig. 4

EXTERNAL DISTRIBUTION IN ADDITION TO UC-420

Dr. F. Paoloni, Univ. of Wollongong, AUSTRALIA
Prof. M.H. Brennan, Univ. of Sydney, AUSTRALIA
Plasma Research Lab., Australian Nat. Univ., AUSTRALIA
Prof. I.R. Jones, Flinders Univ, AUSTRALIA
Prof. F. Cap, Inst. for Theoretical Physics, AUSTRIA
Prof. M. Heindler, Institut für Theoretische Physik, AUSTRIA
Prof. M. Goossens, Astronomisch Instituut, BELGIUM
Ecole Royale Militaire, Lab. de Phy. Plasmas, BELGIUM
Commission-European, DG. XII-Fusion Prog., BELGIUM
Prof. R. Boucique, Rijksuniversiteit Gent, BELGIUM
Dr. P.H. Sakanaka, Instituto Fisica, BRAZIL
Instituto Nacional De Pesquisas Espaciais-INPE, BRAZIL
Documents Office, Atomic Energy of Canada Ltd., CANADA
Dr. M.P. Bachynski, MPB Technologies, Inc., CANADA
Dr. H.M. Skarsgard, Univ. of Saskatchewan, CANADA
Prof. J. Teichmann, Univ. of Montreal, CANADA
Prof. S.R. Sreenivasan, Univ. of Calgary, CANADA
Prof. T.W. Johnston, INRS-Energie, CANADA
Dr. R. Bolton, Centre canadien de fusion magnétique, CANADA
Dr. C.R. James,, Univ. of Alberta, CANADA
Dr. P. Lukác, Komenského Universzita, CZECHO-SLOVAKIA
The Librarian, Culham Laboratory, ENGLAND
Library, R61, Rutherford Appleton Laboratory, ENGLAND
Mrs. S.A. Hutchinson, JET Library, ENGLAND
Dr. S.C. Sharma, Univ. of South Pacific, FIJI ISLANDS
P. Mähönen, Univ. of Helsinki, FINLAND
Prof. M.N. Bussac, Ecole Polytechnique,, FRANCE
C. Mouttet, Lab. de Physique des Milieux Ionisés, FRANCE
J. Radet, CEN/CADARACHE - Bat 506, FRANCE
Prof. E. Economou, Univ. of Crete, GREECE
Ms. C. Rinni, Univ. of Ioannina, GREECE
Dr. T. Mual, Academy Bibliographic Ser., HONG KONG
Preprint Library, Hungarian Academy of Sci., HUNGARY
Dr. B. DasGupta, Saha Inst. of Nuclear Physics, INDIA
Dr. P. Kaw, Inst. for Plasma Research, INDIA
Dr. P. Rosenau, Israel Inst. of Technology, ISRAEL
Librarian, International Center for Theo Physics, ITALY
Miss C. De Palo, Associazione EURATOM-ENEA , ITALY
Dr. G. Grosso, Istituto di Fisica del Plasma, ITALY
Prof. G. Rostangni, Istituto Gas Ionizzati Del Cnr, ITALY
Dr. H. Yamato, Toshiba Res & Devel Center, JAPAN
Prof. I. Kawakami, Hiroshima Univ., JAPAN
Prof. K. Nishikawa, Hiroshima Univ., JAPAN
Director, Japan Atomic Energy Research Inst., JAPAN
Prof. S. Itoh, Kyushu Univ., JAPAN
Research Info. Ctr., National Instit. for Fusion Science, JAPAN
Prof. S. Tanaka, Kyoto Univ., JAPAN
Library, Kyoto Univ., JAPAN
Prof. N. Inoue, Univ. of Tokyo, JAPAN
Secretary, Plasma Section, Electrotechnical Lab., JAPAN
S. Mori, Technical Advisor, JAERI, JAPAN
Dr. O. Mitarai, Kumamoto Inst. of Technology, JAPAN
J. Hyeon-Sook, Korea Atomic Energy Research Inst., KOREA
D.I. Choi, The Korea Adv. Inst. of Sci. & Tech., KOREA
Prof. B.S. Liley, Univ. of Waikato, NEW ZEALAND
Inst of Physics, Chinese Acad Sci PEOPLE'S REP. OF CHINA
Library, Inst. of Plasma Physics, PEOPLE'S REP. OF CHINA
Tsinghua Univ. Library, PEOPLE'S REPUBLIC OF CHINA
Z. Li, S.W. Inst Physics, PEOPLE'S REPUBLIC OF CHINA
Prof. J.A.C. Cabral, Instituto Superior Tecnico, PORTUGAL
Dr. O. Petrus, AL I CUZA Univ., ROMANIA
Dr. J. de Villiers, Fusion Studies, AEC, S. AFRICA
Prof. M.A. Hellberg, Univ. of Natal, S. AFRICA
Prof. D.E. Kim, Pohang Inst. of Sci. & Tech., SO. KOREA
Prof. C.I.E.M.A.T, Fusion Division Library, SPAIN
Dr. L. Stenflo, Univ. of UMEA, SWEDEN
Library, Royal Inst. of Technology, SWEDEN
Prof. H. Wilhelmson, Chalmers Univ. of Tech., SWEDEN
Centre Phys. Des Plasmas, Ecole Polytech, SWITZERLAND
Bibliotheek, Inst. Voor Plasma-Fysica, THE NETHERLANDS
Asst. Prof. Dr. S. Cakir, Middle East Tech. Univ., TURKEY
Dr. V.A. Glukhikh, Sci. Res. Inst. Electrophys.I Apparatus, USSR
Dr. D.D. Ryutov, Siberian Branch of Academy of Sci., USSR
Dr. G.A. Eliseev, I.V. Kurchatov Inst., USSR
Librarian, The Ukr.SSR Academy of Sciences, USSR
Dr. L.M. Kovrizhnykh, Inst. of General Physics, USSR
Kernforschungsanlage GmbH, Zentralbibliothek, W. GERMANY
Bibliothek, Inst. Für Plasmaforschung, W. GERMANY
Prof. K. Schindler, Ruhr-Universität Bochum, W. GERMANY
Dr. F. Wagner, (ASDEX), Max-Planck-Institut, W. GERMANY
Librarian, Max-Planck-Institut, W. GERMANY
Prof. R.K. Janev, Inst. of Physics, YUGOSLAVIA

END

DATE
FILMED
9 /24/92